

Pancreas-Specific ARID1A Deficiency Promotes Acinar-to-Ductal Metaplasia and Elevates Interleukin-6 Expression in Experimental Pancreatitis Model

Liming Zhang

Taizhou Central Hospital(Taizhou University Hospital)

Zhaoyun Li

Taizhou Central Hospital(Taizhou University Hospital)

Yong Zhou

Taizhou Central Hospital(Taizhou University Hospital)

Jie Zhu

Taizhou Central Hospital(Taizhou University Hospital)

Chong Jin

Taizhou Central Hospital(Taizhou University Hospital)

Jing-gang Mo (✉ mojg@tzzxyy.com)

Taizhou University <https://orcid.org/0000-0003-3538-4326>

Primary research

Keywords: Arid1a deficiency, SWI/SNF complex, acinar-to-ductal metaplasia, acute pancreatitis, IL-6, epigenetic regulation

Posted Date: April 12th, 2021

DOI: <https://doi.org/10.21203/rs.3.rs-326796/v1>

License:   This work is licensed under a Creative Commons Attribution 4.0 International License.

[Read Full License](#)

Abstract

Background: Although role of ARID1A in pancreatic homeostasis and tumorigenesis has been recently described using genetically engineered mouse (GEM) models, whether ARID1A plays a role in pancreatic inflammation and regeneration remains to be explored.

Methods: Pancreas-specific *Arid1a*-deficient GEM model (*Arid1a*^{def}) was generated by *Ela1-Cre/ERT2* mice crossing with *Arid1a*^{fl/fl} mice and characterized histologically. In physiological and inflammatory conditions, serum amylase and lipase activity were measured to investigate effects of *Arid1a* deficiency on pancreatic secretion function. Histology analysis of pancreas was used to evaluate pancreatic lesions and recovery. *Ex vivo* primary acinar cell culture was employed to study acinar-to-ductal metaplasia (ADM) process. In HPNE cells, ARID1A knockdown and histone acetyltransferases inhibitors were used to explore epigenetic regulation on interleukin-6 (IL6) expression. Chromatin immunoprecipitation (ChIP) and quantitative real-time PCR were performed to analyze on IL6 promoters.

Results: *Arid1a* deficiency promoted formation of ductal cysts characterized as silenced acinar genes and activated duct genes. *Arid1a*-deficient acinar cells were more inclined to trans-differentiation to ductal cells in cerulein-induced acute pancreatitis (AP) model. Expression analysis of proinflammatory cytokines reveals that ARID1A deficiency led to increased IL-6 expression in mice acinar cells and HPNE cells. ARID1A-associated histone acetylation partially involved in epigenetic regulation of IL-6.

Conclusion: These results demonstrate ARID1A is involved in cerulein-induced AP development by mediating pro-inflammatory cytokines IL-6 and suggest that ARID1A-containing SWI/SNF complex is an epigenetic regulator of acute pancreatitis.

Background

Pancreatitis is an inflammatory disease of highly variable severity, beginning with an injury to the pancreas and resulting in an inflammatory response [1]. Genetically engineered mouse models (GEMM) can be a useful tool to study the pathophysiology of pancreatitis. During the inflammatory cascade, response genes seem to be activated by signaling molecules or cytokines [2]. In addition to intricate balance between proinflammatory cytokine (IL-1beta, TNF-alpha, IL-6, IL-8, and platelet activating factor) and anti-inflammatory cytokine (IL-10, TNF-soluble receptors and IL-1 receptor antagonist) [3], epigenetic control mechanisms are being attached great importance in the control of the inflammatory cascade. Chromatin remodeling complex are associated with epigenetic regulation of both early and late proinflammatory genes in acute pancreatitis, therefore play an important role in the control of the inflammatory cascade [4]. Chromatin remodeling complexes are a group of epigenetic regulators that play a key role in orchestrating chromatin architecture and gene expression by directly altering the assembly of nucleosomes as well as the accessibility of transcription factor to DNA. In particular, the SWI/SNF complex control transcription by activating promoter/enhancer regions by partially regulating acetylated histone H3K27 (K3K27ac) [5, 6], where histone acetylation marks are catalyzed by histone

acetyltransferases (HATs) and histone deacetylases (HDACs). More importantly, HATs and HDACs play a central role in transcriptional regulation of genes involved in the inflammatory response [7, 8].

ARID1A, a component of SWI/SNF chromatin remodeling complex, has been shown to play important roles in tissue homeostasis and regeneration. ARID1A is the most frequently mutated at variable frequencies across molecular and histological subtypes of cancer [9–11]. Within the context of functional models *in vitro* and *in vivo*, ARID1A was involved in multiple biological processes, such as proliferation, differentiation, senescence, apoptosis, metastasis, and angiogenesis [12–17]. Intriguingly, several investigations reveal important roles of ARID1A inactivation in inflammation-driven tumorigenesis. In human ovarian tissue, ARID1A mutations seem to be an important early event in the malignant transformation of endometriosis to endometrioid and clear cell carcinomas [18]. It is noteworthy that ARID1A inactivation in cooperation with PIK3CA activation promote tumorigenesis through pro-tumorigenic inflammatory cytokine signaling, and proposed that ARID1A protects against inflammation-driven tumorigenesis [19]. In addition, hepatocyte-specific Arid1a knockout could result in mouse steatohepatitis and tumor development [20]. ARID1A plays important roles in tissue homeostasis and regeneration [21–23]. Nevertheless, it remains unclear whether ARID1A deficiency is implicated in pancreatitis and tissue regeneration after injury. Interleukin 6 (IL-6), as a multifunctional cytokine, is closely linked to the most burdened exocrine pancreatic diseases including acute pancreatitis, chronic pancreatitis and pancreatic cancer [24]. Epigenetic mechanisms influencing IL-6 expression in acute pancreatitis are poorly understood.

Notably, our previous study *in vitro* suggests that ARID1A knockdown promotes malignant transformation through inhibiting oncogene-induced senescence in human pancreatic cell lines [16]. Furthermore, evidences from both mice PDAC and pancreatitis patients display pancreatitis-induced inflammation can inhibit oncogene-induced senescence [25], prompting us to hypothesize that ARID1A functions in inflammation during pancreatic lesions. Pancreatic acinar cells are with high plasticity, and have capability to dedifferentiate or transdifferentiate to a progenitor-like phenotype that express ductal markers, in a process termed acinar-to-ductal metaplasia (ADM) during pancreatic inflammation or injury in mouse and human tissue [26]. The present work focuses on acute pancreatitis as an experimental model of acute inflammation. In this study, we investigated the roles of Arid1a deficiency in mice pancreas under physiological condition and cerulein-induced acute pancreatitis using a conditional acinar-specific Arid1a knockout mice model. We further observed the effect of Arid1a deficiency on ADM, proinflammatory cytokines, and epigenetic regulatory mechanisms in the control of the inflammatory cascade. Our findings highlight ARID1A-mediated epigenetic regulation on inflammatory response and provide an anti-inflammation approach based on epigenetic inhibitors targeting against ARID1A deficient patients.

Materials And Methods

Generation of conditional acinar-specific loss of Arid1a Mice

Arid1a^{fl/fl} floxed mice have loxP sites Jackson Laboratory (Stock No: 027717) were bred to *Ela1-Cre/ERT2* transgenic mice (Stock No: 008861) to generate *Arid1a*^{fl/fl}; *Ela1-Cre/ERT2* mice. *Ela1-Cre/ERT2* have a tamoxifen-inducible Cre-mediated recombination system driven by the rat elastase 1 pancreatic promoter. All mice were housed in pathogen-free animal facilities and handled in accordance with the guidelines of the Institutional Animal Care and Use Committee at Taizhou University Hospital. Cre recombinase activity was induced by daily intraperitoneal injection of tamoxifen (Sigma-Aldrich, St. Louis, MO) over five days. *Arid1a*^{fl/fl}; *Ela1-Cre/ERT2* mice were administered tamoxifen at a dose of 0.25mg/g body weight or equivalent corn oil. Excision of *Arid1a* was evaluated in mice 1 week after injection by PCR of DNA collected from mouse tissues. Primers of PCR genotyping were listed in **Supplementary Table 1**.

Cerulein-induced acute pancreatitis (AP)

1 week after the mice were administrated with tamoxifen, acute pancreatitis (AP) was induced by intraperitoneal injections of cerulein (Sigma-Aldrich, Steinheim, Germany) eight times hourly for two consecutive days with a total of 0.1 µg/g body weight per mouse, as previously described [27]. The final day of injection was considered as day 0. Blood was collected at 1, 3, 5, 10 hours, 1, 5 and 7 days after the last cerulein injection to examine the serum amylase and lipase levels.

Tissue processing and histology

Mice were euthanized at indicated time points, pancreata were dissected in ice-cold PBS and separated into multiple fragments. Formalin-fixed, paraffin-embedded (FFPE) pancreas tissue was cut into 6-8 µm sections and stained with H&E. Pancreatic damage was semi-quantitatively assessed by scoring 3-5 random slides per mouse according to quantitative method described in the references [28-30]. Briefly, the semi-quantitative scoring system for edema and acinar necrosis were graded from 0 to 3 according to the following criteria: edema: 0, absent; 1, focally increased between lobules; 2, diffusely increased between lobules; and 3, acini disrupted and separated; and acinar necrosis: 0, absent; 1, periductal necrosis (5%); 2, focal necrosis (5-20%); and 3, diffuse parenchymal necrosis (20-50%). Total pancreatitis was calculated by grade of inflammation × distribution of inflammation. The scoring was performed in a blinded manner by an experienced pathologist.

Serological examination of amylase, lipase, and IL-6 cytokine

The serum activity of amylases and lipases were measured by enzyme dynamics chemistry using commercial kits, according to the manufacturer's instructions in a Roche/Hitachi modular analytics system (Roche, Mannheim, Germany). Serum IL-6 level was determined by enzyme-linked immunosorbent assay (ELISA) using a commercial kit (Quantikine; R&D Systems, Minneapolis, MN, USA).

Immunohistochemistry and immunofluorescence assay

FFPE samples were cut into 5µm sections. After deparaffinization and rehydration by passage through xylene and a graded alcohol series, heat-induced antigen retrieval was achieved by cooking in antigen

unmasking solution (Vector Laboratories). Endogenous peroxidase activity was inactivated by 0.3% hydrogen peroxide treatment for 10 min at room temperature. After blocking with TBS containing 3% BSA, sections were incubated with the primary antibody at 4 °C overnight. For immunohistochemistry, sections were incubated in secondary antibody for 1 hour and then developed using Avidin-Biotin Complex (ABC) and Diaminobenzidine (DAB) kit (Vector Laboratories) and counterstained with hematoxylin. For immunofluorescence assay, slides were subject to primary and secondary antibody incubations, counterstained with DAPI (Sigma-Aldrich; St. Louis, MO).

Isolation and culture of primary acinar cells

Primary acinar cells were isolated from mice pancreas using a collagenase digestion as previously described procedure [31, 32]. Briefly, pancreata were immediately removed and rinsed twice with ice-cold Hank's Balanced Salt Solution (HBSS, Thermo Fisher Scientific). Pancreatic tissue was minced into 1-5 mm pieces and digested with collagenase P (Roche Applied Science, Mannheim, Germany) for 15 min at 37 °C. Isolated acini were washed three times in ice-cold HBSS containing 5% fetal bovine serum (FBS), and then filtered through 500 and 105- μ m nylon meshes (Spectrum Laboratories, CA, USA). Acini were collected by centrifugation and re-suspend in 10 ml Waymouth medium (Invitrogen, Carlsbad, USA) containing 1% FBS, 0.1 mg/ml soybean trypsin inhibitor, 1 μ g/ml dexamethasone. Culture dishes were coated with rat tail collagen type I (Sigma-Aldrich) in 0.02 N acetic acid, pH 3.67 solution for 1 hr at 37 °C, and the isolated primary acini were seed into the prepared plates coated with matrix scaffolds in triplicates. Acinar cells were infected with lentivirus of interest and incubated for 3-5 hours before embedding in the collagen/waymouth media mixture. Numbers of ducts were counted under a microscope. Acinar explants were seeded in triplicates, and cells clusters were counted from at least 3 optical fields/well and reported as a percentage of acinar clusters and ring-like spheres.

RNA isolation and reverse transcription quantitative-PCR (RT-qPCR)

Total mRNA was isolated using Trizol reagent (Ambion) following manufacture's instruction. 1 μ g RNA was reverse transcribed using oligo dT primer was performed with iScriptTM gDNA Clear cDNA Synthesis Kit (BIO-RAD). Synthesized cDNAs were diluted 2-fold with water, and regions of interest were amplified by SYBR[®] Green Real-Time PCR Master Mixes (Thermo Fisher Scientific). Ct values of target genes were normalized using that of housekeeping geneGapdh. In addition, we employed a reference gene Rpl13a used for normalization in qRT-PCR analyses in AP mouse tissue [33]. The primer sequences used in the study are listed in **Supplementary Table 1**.

Flow cytometric analysis of cell proliferation and apoptosis

Cell apoptosis was detected using the Annexin V-FITC/PI Apoptosis Detection Kit (BD Biosciences) following the manufacturer's instructions. Briefly, the cells were collected and suspended in binding buffer, followed by incubation with Annexin V-FITC and PI. The stained samples were loaded on FACSCalibur flow cytometer (BD Biosciences) and produced data were analyzed with CELLQuest

software (BD Biosciences). Cell proliferation was analyzed using Click-iT® Plus Edu Proliferation Kits (ThermoFisher) according to the manufacturer's protocol.

ChIP-qPCR

Chromatin immunoprecipitation (ChIP) was performed using the EZ ChIP™ Chromatin Immunoprecipitation Kit (Merck Millipore, Billerica, MA, USA) according to the manufacturer's instruction. Cells were cross-linked with 1% formaldehyde for 15 min and quenched using 125 mM glycine for 5 min. Sonication was performed by three runs of 10 cycles (30 s "ON", 30 s "OFF") at high power setting (Bioruptor, Diagenode). Chromatin lysates were immunoprecipitated with anti-H3K27ac (ab4729, Abcam). Real-time quantitative PCR was using PCR master mix (Bio-Rad) and specific primers for regulatory elements regions of human IL-6 listed in **Supplementary Table 1**.

Western Blot Assay

The primary antibodies used for Western blotting are as following: ARID1A (1:1000, Cell Signaling, #12354), IL-6 (1:1000, Abcam, ab6672), and β -actin (1:5000, Santa Cruz, AC-15). After incubation with peroxidase-conjugated secondary antibodies, membranes were developed using the enhanced chemiluminescent immunoassay for the detection of antigen.

Statistical Analysis.

All data from mice experiments are shown as means \pm SEM. Statistical comparisons were performed by the two-tailed Student's t-test. Analyses were performed using GraphPad Software (San Diego, CA, USA). $p < 0.05$ was considered statistically significantly.

Results

Conditional Arid1a deficiency in mature acinar compartment had no detectable effects on pancreatic function

To determine whether Arid1a deficiency contributes to pancreatic pathogenesis, we generated a tamoxifen-inducible pancreas-specific Arid1a-deficient GEM model driven by *Ela1-Cre/ERT2* targeting acinar cells only (See Methods). To induce Cre-mediated excision of *Arid1a* exon, mice aged 6–8 weeks were intraperitoneally injected with tamoxifen (Tam), and then mice were sacrificed at 9-week and 40-week to harvest pancreata and blood samples, respectively (Fig. 1a). We first evaluated efficiency of Cre-mediated *Arid1a* depletion at 1-week post-Tam treatment. Genotyping analysis of *Arid1a* alleles showed the 268-bp fragment of excised Arid1a loci was present in pancreata tissue of *Arid1a^{fl/fl}; Ela1-Cre/ERT2* mice with Tam treatment, while only floxed-*Arid1a* alleles were observed in tail and pancreata samples of control mice injected with corn oil (vehicle control) (Figure S1a). Moreover, Arid1a protein was obviously

decreased when bulk pancreata were examined by western blotting (Figure S1b). Henceforth, *Arid1a^{fl/fl}; Ela1-Cre/ERT2* mice injected with tamoxifen were referred to as *Arid1a^{def}*; their counterpart treated with corn oil were designated as *Arid1a^{+/+}*. *Arid1a^{def}* mice survived healthily until euthanasia when 40-week-old and exhibited normal body weight. During this time, no signs of any insufficiency in the pancreatic exocrine functions were found in *Arid1a^{+/+}* and *Arid1a^{def}* mice, such as weight loss (Fig. 1b). Moreover, the pancreas/body weight ratio was not significantly different between the two groups of mice (Fig. 1c) at the 9-week ($p = 0.485$) and 40-week ($p = 0.962$) time points. Histologically, H&E analysis revealed no obvious difference in tissue structure of the pancreas between two groups (Fig. 1d). To further address the role of *Arid1a* gene in exocrine function of acinar cells, we examined amylase and lipase secretion *in vivo* over the course of specified time periods respectively. The blood amylase activity analysis showed no difference in serum amylase between *Arid1a^{+/+}* and *Arid1a^{def}* mice at the 9-week ($p = 0.622$) and 40-week ($p = 0.790$) time points (Fig. 1e). In addition, we did not observe significant difference of serum lipase between the two groups of mice at the 9-week ($p = 0.883$) and 40-week ($p = 0.858$) time points (Fig. 1f). Taken together, these results demonstrated that *Arid1a* deficiency in mature acinar cells had no obvious effects on pancreatic exocrine function.

Arid1a deficiency promoted ADM formation upon TGF α or Cerulein (Cer) treatment

During pancreas injury or inflammation, a reversible ADM metaplasia occurs and deservedly contributes to the regeneration of acinar structures [26]. Since ADM represents a cellular mechanism accounting for regeneration after inflammation or injury, thus we hypothesized that *Arid1a* plays a role in pancreatic epithelial plasticity mediated by acinar cell metaplasia. We employed *ex vivo* primary acini culture system to investigate the ADM process. To determine whether *Arid1a* deficiency contributes to ADM, we initially utilized a defined explant model [34, 35], in which acinar cells were seeded in collagen-coated plates and treated with TGF α to induce acinar trans-differentiation. First, we observed ADM of *Arid1a^{fl/fl}* mouse primary acinar cells that were lentivirally-infected with GFP or Cre. Floxed-*Arid1a* exon were fully excised and *Arid1a* protein obviously decreased (Figure S2a), and TGF α -induced formation of ductal structure was significantly increased to approximately 60% when *Arid1a* was excised by Cre (Figure S2b, $p < 0.01$). Furthermore, acini were also isolated from *Arid1a^{+/+}* and *Arid1a^{def}* mice, and *Arid1a* deficiency not only had effects on the numbers of ducts formed, but also affected their size (Fig. 2a, $p < 0.01$). To further confirm acinar conversion to ductal phenotype, we analyzed expression profiling of acinar and ductal genes using quantitative PCR analysis. When acinar cells were treated with TGF α for 5 days, *Arid1a^{def}* cells displayed downregulated expression of acinar markers (Amylase, Lipase, Cpa1, Mist1, and Ptf1a) and upregulated expression of ductal genes (Cftr, Krt19, Call, Nes, Sox9, and Hnf6) compared with *Arid1a^{+/+}* controls (Fig. 2b). As demonstrated by western blotting assay, the expression of amylase decreased whereas CK-19 remarkably increased in these *Arid1a*-deficient cells (Fig. 2c). Thus, these results suggest *Arid1a* deficiency promote ADM formation of primary acinar cell. To validate whether *Arid1a* deficiency contributes to ADM *in vivo*, we observed effects of *Arid1a* deficiency on ADM in acute pancreatitis (AP) model induced by Cer. Significantly, *Arid1a* deficiency promoted ADM formation of acinar cells in the AP model, as shown by quantitative analysis of H&E staining (Fig. 2d, $p < 0.01$) and IHC

assay for CK-19 staining (Fig. 2e, $p < 0.05$). Taken together, these data indicate that Arid1a acts as a critical epigenetic mediator to facilitate metaplasia of acinar cells under the context of pancreas injury.

Arid1a deficiency influenced cell proliferation and exocrine secretion of acinar cells

Amylase and lipase levels derived from pancreatic acinar cells are important index as a reflection of acinar cell function and pancreas regeneration after injury [3, 36]. We measured serum amylase and lipase levels at various time points for the AP model, and dynamic monitoring showed a decreasing trend in both amylase and lipase levels of Arid1a^{def} mice over the course of time (Fig. 3a), although significant differences of amylase levels between two groups were statistically present at 10-hour ($p < 0.01$) and 24-hour ($p < 0.05$) time points after Cer treatment. In contrast, Arid1a deficiency sustained significant reduced level of lipase at these time points from 10-hour until 7-day (Fig. 3b, 5-day, $p < 0.01$; 10-hour, 1-day and 7-day, $p < 0.05$). To observe distribution and degree of histologic lesions, we applied a defined scoring system [29, 37] to evaluate tissue injury and regeneration of the AP model. As a result, no significant differences between the two groups could be observed in the pancreas weight and edema (Figure S3a-b). However, Arid1a-deficient acinar cells showed lower grade of necrosis, and a significant decrease of necrosis was observed at the 5th day of AP injury/regeneration model (Figure S3c). Arid1a-deficient mice somehow displayed strong pancreatitis as compared with Arid1a^{+/+} mice, even though quantification assessment of the pancreatitis exhibited a significant increase at 3h after cerulein treatment (Figure S3d). In sum, these histological analysis based on the scoring system were multifactorial and various in the severity of acute pancreatitis [38], which was difficult to unveil Arid1a's exact roles in murine AP model. To further observe effect of Arid1a deficiency on cell proliferation, we performed immunofluorescence for Ki-67 on AP tissue and EdU cell proliferation assays in primary explant culture of primary acinar cells. Significantly, Arid1a-deficient led to a 2-fold increase of Ki-67 positive cells found in AP tissues (Fig. 3c, $p < 0.01$). Furthermore, we evaluated cell proliferation when primary acinar cells were treated with 10 μ M Edu for 3 hours. Flow cytometry assay showed that cells labeled by Edu were $28.3 \pm 1.5\%$ in primary acinar cells isolated from Arid1a^{+/+} mice at 3 independent experiments, whereas Edu-labeling cells were $37.1 \pm 2.2\%$ and significantly increased in cultured acinar cells from Arid1a^{def} mice (Fig. 3d, $p < 0.01$). Taken together, these results implied that Arid1a deficiency partly impaired pancreatic exocrine function and promoted cellular proliferation under the pathological condition of acute pancreatic injury.

Arid1a deficiency led to enriched histone H3K27ac modification on IL-6 gene

To gain insight into the molecular mechanisms how Arid1a was involved in pancreatic inflammatory response, we analyzed cytokine expression levels in AP tissue. We performed qRT-PCR on a subset of cytokine genes, including proinflammatory cytokines IL-6, Ifn γ , Tnf α , Lbp, G-Csf, Ifn α , IL-1 α , IL-1 β , as well as anti-inflammatory cytokines IL-10, IL-13, Tgf β , Csf. Among these cytokines examined, IL-6 and IL-10 mRNA were found to be significantly elevated in Arid1a^{def} mice, however no significant differences were found for other cytokines examined (Fig. 4a-b, *, $p < 0.05$; **, $p < 0.01$). Since IL-6 is strongly linked to the most burdened exocrine pancreatic diseases including acute pancreatitis, chronic pancreatitis and pancreatic cancer [24], we next try to address epigenetic mechanism of IL-6 regulation associated with

Arid1a deficiency in inflammatory cytokine signaling. Quantitative analysis of serum IL-6 indeed supported that Arid1a deficiency increased serum level of IL-6 *in vivo* (Fig. 4c, **, $p < 0.01$).

To further validate the role of ARID1A deficiency in mediating IL-6 transcription, we established isogenic cell models which were derived from human HPNE with KRAS mutant (*KRAS*^{G12D}) as well as CRISPR/Cas9-mediated ARID1A knockout. We identified ARID1A wildtype (WT) and knockout (KO) subclones derived from single cell, 2 WT and 2 KO subclones were used to study ARID1A-associated regulatory effects on IL-6. Activation of the p42/p44 (Erk1/2) MAP kinase (MAPK) phosphorylation cascade, a major downstream effector of KRAS signaling as well as ARID1A knockout were confirmed by western blot assay (Fig. 5a). ARID1A knockout notably increased IL-6 expression at protein and mRNA level (Fig. 5a-b), supporting that upregulation of IL mediated by loss of ARID1A function can be reproduced in this context of human cells. According to these observations, we hypothesized that ARID1A deficiency remodels H3K27ac status on IL-6 gene locus. To test this hypothesis, we first analyzed the H3K27ac ChIP-seq datasets in 7 available human cell lines using a website tool from ENCODE at UCSC (<https://genome.ucsc.edu/encode/>). We found that H3K27ac binding sites conservatively enriched in the IL6 proximal and distal regions (Figure S4a). Subsequently, we performed ChIP using H3K27ac antibody, and qPCR analysis revealed that a significant enrichment of H3K27 acetylation at the IL-6 distal regions upon ARID1A knockout (Fig. 5c). As known, histone acetylation regulation is specifically controlled by histone deacetylases (HDACs) and histone acetyltransferases (HATs). Histone acetylation by HAT activates inflammatory genes, whereas increased HDAC activity represses inflammatory genes [39], which implies HATs play a leading role in the H3K27 acetylation enrichment on IL-6 gene. Thus, we employed CBP30 and JQ1, two common HAT inhibitors, to inhibit the catalytic activity of HATs [40, 41]. Expectedly, HAT inhibition led to a significant reverse IL-6 expression in ARID1A knockout subline cells relative to wildtype cells (Fig. 5d and Figure S4b, **, $p < 0.01$). Collectively, these results demonstrated that ARID1A knockout remodeled HATs-mediated histone acetylation on IL-6 gene, and thus elevated IL-6 expression.

Discussion

Epigenetic mechanisms, especially chromatin remodeling plays an emerging role in inflammation. Acute pancreatitis is a common digestive disease, and its onset is triggered by acinar events that induce autodigestion and acinar cell injury [42]. Inflammatory processes have emerged as critical regulators of pancreatic tumorigenesis, and induction of pancreatitis accelerates PDAC development. Recurrent acute pancreatitis seems to increase the risk for developing pancreatic cancer. Epigenetic markers such as histone acetylation and methylation, as well as recruitment of SWI/SNF remodeling complex are associated with the upregulation with the upregulation of both early and late proinflammatory genes in acute pancreatitis [4]. As a subunit of the SWI/SNF chromatin remodeling complex, ARID1A is thought to impose upon the genetic code a chromatin structure characterized by chromatin accessibility, nucleosome position, and histone modification [10]. As known, ARID1A was recurrently found to be inactivated in human pancreatic ductal adenocarcinoma (PDAC). In this study, we revealed that Arid1a

deficiency promoted endows acinar cells with more plasticity to stand up against pancreas injury. and enhanced pancreatitis-associated inflammation response through increased H3K27ac-mediated IL-6 expression, Recent studies have shown that role of ARID1A in tumorigenesis is highly dependent upon context, based on genetically engineered mouse (GEM) models. For instance, a hepatocyte specific Arid1a knockout mouse model showed Arid1a deficiency were resistant to tumor initiation while ARID1A overexpression accelerated initiation. In contrast, Arid1a loss in established tumors accelerated progression and metastasis [17]. Another study revealed the paradoxical role of Arid1a in a mouse model with pancreas-specific Arid1a loss [43], supporting the protective role of Arid1a deficiency in pancreatic injury. Inflammation contributes to mouse PDAC, and therefore anti-inflammatory treatment may reduce the risk of developing PDAC [25]. Significantly, Interleukin 6 (IL-6) was acknowledged to participate in cell growth, differentiation and function adjustment and play a vital role in the inflammatory response and tumor growth in a paracrine fashion. IL-6 is required for the maintenance and progression of pancreatic cancer, therefore inhibition of IL-6 may have therapeutic potential for treatment of pancreatic cancer [44].

Acetylation of histone is associated with an “open” chromatin conformation representing activation of transcription, and Apparently, increased histone acetyltransferase activity or enriched local binding of regulatory elements will increase histone acetylation, leading to transcriptional activation. For example, the promoters of several pro-inflammatory cytokines (IL-1,IL-2, IL-8, and IL-12) were acetylated by CBP/p300, so that the cytokines are rapidly induced to response for inflammation[8]. In the study, we demonstrated that ARID1A could bind to distal and proximal regulatory elements of IL-6 gene, and thus affect their acetylation modification due to alternations of chromatin accessibility. Together, these evidences uncovered that epigenetic regulatory mechanism of IL-6 in pancreatic acinar cells. Hence, inhibition of IL-6 may have therapeutic potential for treatment of cancers characterized by oncogenic Ras mutations [45]. More practically, the highly selective inhibitors of the bromodomains of CBP/p300, JQ1 and CBP30, successfully inhibited IL-6 expression in human HPNE cells. recent investigation in macrophages demonstrated the increased binding of p300HAT to the promoter regions of IL-6 could elevate gene transcription through acetylation of histone [46], implying a regulatory role of p300 in H3K27ac at the IL-6 gene. The results demonstrated that Arid1a deficiency promoted ADM when acinar cells were stimulated by cerulein or inflammatory signaling. Mechanistically, Arid1a deficiency led to increased H3K27ac modification on IL-6 distal region to partially elevate its transcription. More importantly, we propose that the epigenetic inhibitors have considerable promise for the treatment of ARID1A-deficient pancreatic inflammatory diseases.

Abbreviations

ARID1A

AT-rich interaction domain 1A

PDAC

pancreatic ductal adenocarcinoma

GEMM

genetically engineered mouse models

ADM
acinar-to-ductal metaplasia
ChIP
chromatin immunoprecipitation
AP
Acute pancreatitis
FFPE
Formalin-fixed, paraffin-embedded
ELISA
enzyme-linked immuno sorbent assay
ABC
Avidin-Biotin Complex
DAB
Diaminobenzidine
HBSS
Hank's Balanced Salt Solution
EdU
5-ethynyl-2'-deoxyuridine
FBS
fetal bovine serum
RT-qPCR
reverse transcription quantitative-PCR
Tam
tamoxifen
HDACs
histone deacetylases
HATs
histone acetyltransferases
HPNE
Human Pancreatic Nestin Expressing cells
PI
Propidium Iodide

Declarations

Acknowledgements

Authors appreciated the personnel of the Nanchang University of Laboratory Animal Center for guidance and help.

Authors' contributions

LMZ, ZYL, YZ, JZ, CJ, performed the experiments. JGM supervised the study. All authors read and approved the final manuscript.

Funding

This work was supported by research grants from the Taizhou Science and Technology Bureau(1901ky38), Zhejiang Provincial Health Commission(2020ky1054), and Zhejiang Science and Technology Department (LGC20H200004).

Availability of data and materials

The data used during the current study are available from the corresponding author upon reasonable request.

Ethical approval and consent to participate

All procedures performed in the study involving animals were in accordance with the guidelines of the Institutional Animal Care and Use Committee at Taizhou University Hospital.

Competing interests

The authors declare that they have no competing interests.

References

1. Walling A, Freelove R. Pancreatitis and Pancreatic Cancer. *Prim Care*. 2017;44(4):609–20.
2. Smale ST. Selective transcription in response to an inflammatory stimulus. *Cell*. 2010;140(6):833–44.
3. Granger J, Remick D. Acute pancreatitis: models, markers, and mediators. *Shock*. 2005;24(Suppl 1):45–51.
4. Sandoval J, Pereda J, Perez S, Finamor I, Vallet-Sanchez A, Rodriguez JL, Franco L, Sastre J, Lopez-Rodas G. Epigenetic Regulation of Early- and Late-Response Genes in Acute Pancreatitis. *J Immunol*. 2016;197(10):4137–50.
5. Mathur R, Alver BH, San Roman AK, Wilson BG, Wang X, Agoston AT, Park PJ, Shivdasani RA, Roberts CW. ARID1A loss impairs enhancer-mediated gene regulation and drives colon cancer in mice. *Nat Genet*. 2017;49(2):296–302.
6. Wang X, Lee RS, Alver BH, Haswell JR, Wang S, Mieczkowski J, Drier Y, Gillespie SM, Archer TC, Wu JN, et al. SMARCB1-mediated SWI/SNF complex function is essential for enhancer regulation. *Nat Genet*. 2017;49(2):289–95.
7. Obata Y, Furusawa Y, Hase K. Epigenetic modifications of the immune system in health and disease. *Immunol Cell Biol*. 2015;93(3):226–32.

8. Villagra A, Sotomayor EM, Seto E. Histone deacetylases and the immunological network: implications in cancer and inflammation. *Oncogene*. 2010;29(2):157–73.
9. Kadoch C, Crabtree GR. Mammalian SWI/SNF chromatin remodeling complexes and cancer: Mechanistic insights gained from human genomics. *Sci Adv*. 2015;1(5):e1500447.
10. Wu JN, Roberts CW. ARID1A mutations in cancer: another epigenetic tumor suppressor? *Cancer Discov*. 2013;3(1):35–43.
11. Mathur R. ARID1A loss in cancer: Towards a mechanistic understanding. *Pharmacol Ther*. 2018;190:15–23.
12. Vanderborght B, Lefere S, Vlierberghe HV, Devisscher L. **The Angiopoietin/Tie2 Pathway in Hepatocellular Carcinoma.** *Cells*. 2020 Oct 30;9(11):2382.
13. Zang ZJ, Cutcutache I, Poon SL, Zhang SL, McPherson JR, Tao J, Rajasegaran V, Heng HL, Deng N, Gan A, et al. Exome sequencing of gastric adenocarcinoma identifies recurrent somatic mutations in cell adhesion and chromatin remodeling genes. *Nat Genet*. 2012;44(5):570–4.
14. Gao X, Tate P, Hu P, Tjian R, Skarnes WC, Wang Z: **ES cell pluripotency and germ-layer formation require the SWI/SNF chromatin remodeling component BAF250a.** *Proceedings of the National Academy of Sciences of the United States of America* 2008, **105**(18):6656–6661.
15. Luo B, Cheung HW, Subramanian A, Sharifnia T, Okamoto M, Yang X, Hinkle G, Boehm JS, Beroukhir R, Weir BA, et al. Highly parallel identification of essential genes in cancer cells. *Proc Natl Acad Sci USA*. 2008;105(51):20380–5.
16. Li ZY, Zhu SS, Chen XJ, Zhu J, Chen Q, Zhang YQ, Zhang CL, Guo TT, Zhang LM. ARID1A suppresses malignant transformation of human pancreatic cells via mediating senescence-associated miR-503/CDKN2A regulatory axis. *Biochem Biophys Res Commun*. 2017;493(2):1018–25.
17. Hu B, Yang XB, Sang XT. **Development of an immune-related prognostic index associated with hepatocellular carcinoma.** *Aging (Albany NY)*. 2020 Mar 19;12(6):5010–5030.
18. Munksgaard PS, Blaakaer J. The association between endometriosis and ovarian cancer: a review of histological, genetic and molecular alterations. *Gynecol Oncol*. 2012;124(1):164–9.
19. Chandler RL, Damrauer JS, Raab JR, Schisler JC, Wilkerson MD, Didion JP, Starmer J, Serber D, Yee D, Xiong J, et al. Coexistent ARID1A-PIK3CA mutations promote ovarian clear-cell tumorigenesis through pro-tumorigenic inflammatory cytokine signalling. *Nat Commun*. 2015;6:6118.
20. Fang JZ, Li C, Liu XY, Hu TT, Fan ZS, Han ZG. Hepatocyte-Specific Arid1a Deficiency Initiates Mouse Steatohepatitis and Hepatocellular Carcinoma. *PloS one*. 2015;10(11):e0143042.
21. Wang W, Friedland SC, Guo B, O'Dell MR, Alexander WB, Whitney-Miller CL, Agostini-Vulaj D, Huber AR, Myers JR, Ashton JM, et al. ARID1A, a SWI/SNF subunit, is critical to acinar cell homeostasis and regeneration and is a barrier to transformation and epithelial-mesenchymal transition in the pancreas. *Gut*. 2019;68(7):1245–58.
22. Peng XQ, Dai SK, Li CP, Liu PP, Wang ZM, Du HZ, Teng ZQ, Yang SG, Liu CM. Loss of Arid1a Promotes Neuronal Survival Following Optic Nerve Injury. *Front Cell Neurosci*. 2020;14:131.

23. Sun X, Chuang JC, Kanchwala M, Wu L, Celen C, Li L, Liang H, Zhang S, Maples T, Nguyen LH, et al. Suppression of the SWI/SNF Component Arid1a Promotes Mammalian Regeneration. *Cell Stem Cell*. 2016;18(4):456–66.
24. Lesina M, Wormann SM, Neuhofer P, Song L, Algul H. Interleukin-6 in inflammatory and malignant diseases of the pancreas. *Semin Immunol*. 2014;26(1):80–7.
25. Guerra C, Collado M, Navas C, Schuhmacher AJ, Hernandez-Porras I, Canamero M, Rodriguez-Justo M, Serrano M, Barbacid M. Pancreatitis-induced inflammation contributes to pancreatic cancer by inhibiting oncogene-induced senescence. *Cancer Cell*. 2011;19(6):728–39.
26. Storz P. Acinar cell plasticity and development of pancreatic ductal adenocarcinoma. *Nat Rev Gastroenterol Hepatol*. 2017;14(5):296–304.
27. Jensen JN, Cameron E, Garay MV, Starkey TW, Gianani R, Jensen J. Recapitulation of elements of embryonic development in adult mouse pancreatic regeneration. *Gastroenterology*. 2005;128(3):728–41.
28. Rongione AJ, Kusske AM, Kwan K, Ashley SW, Reber HA, McFadden DW. Interleukin 10 reduces the severity of acute pancreatitis in rats. *Gastroenterology*. 1997;112(3):960–7.
29. Laukkarinen JM, Van Acker GJ, Weiss ER, Steer ML, Perides G. A mouse model of acute biliary pancreatitis induced by retrograde pancreatic duct infusion of Na-taurocholate. *Gut*. 2007;56(11):1590–8.
30. Schmidt J, Rattner DW, Lewandrowski K, Compton CC, Mandavilli U, Knoefel WT, Warshaw AL. A better model of acute pancreatitis for evaluating therapy. *Ann Surg*. 1992;215(1):44–56.
31. Liou GY, Doppler H, Necela B, Krishna M, Crawford HC, Raimondo M, Storz P. Macrophage-secreted cytokines drive pancreatic acinar-to-ductal metaplasia through NF-kappaB and MMPs. *J Cell Biol*. 2013;202(3):563–77.
32. Sung KF, Odinokova IV, Mareninova OA, Rakonczay Z Jr, Hegyi P, Pandol SJ, Gukovsky I, Gukovskaya AS. Prosurvival Bcl-2 proteins stabilize pancreatic mitochondria and protect against necrosis in experimental pancreatitis. *Exp Cell Res*. 2009;315(11):1975–89.
33. Yan Z, Gao J, Lv X, Yang W, Wen S, Tong H, Tang C. Quantitative Evaluation and Selection of Reference Genes for Quantitative RT-PCR in Mouse Acute Pancreatitis. *BioMed research international*. 2016;2016:8367063.
34. Miyamoto Y, Maitra A, Ghosh B, Zechner U, Argani P, Iacobuzio-Donahue CA, Sriuranpong V, Iso T, Meszoely IM, Wolfe MS, et al. Notch mediates TGF alpha-induced changes in epithelial differentiation during pancreatic tumorigenesis. *Cancer cell*. 2003;3(6):565–76.
35. Means AL, Meszoely IM, Suzuki K, Miyamoto Y, Rustgi AK, Coffey RJ Jr, Wright CV, Stoffers DA, Leach SD. Pancreatic epithelial plasticity mediated by acinar cell transdifferentiation and generation of nestin-positive intermediates. *Development*. 2005;132(16):3767–76.
36. Merry TL, Petrov MS. The rise of genetically engineered mouse models of pancreatitis: A review of literature. *Biomol Concepts*. 2018;9(1):103–14.

37. Nakamichi I, Habtezion A, Zhong B, Contag CH, Butcher EC, Omary MB. Hemin-activated macrophages home to the pancreas and protect from acute pancreatitis via heme oxygenase-1 induction. *J Clin Investig.* 2005;115(11):3007–14.
38. Silva-Vaz P, Abrantes AM, Castelo-Branco M, Gouveia A, Botelho MF, Tralhao JG. **Multifactorial Scores and Biomarkers of Prognosis of Acute Pancreatitis: Applications to Research and Practice.** *Int J Mol Sci* 2020, 21(1).
39. Bayarsaihan D. Epigenetic mechanisms in inflammation. *J Dent Res.* 2011;90(1):9–17.
40. Hammitzsch A, Tallant C, Fedorov O, O'Mahony A, Brennan PE, Hay DA, Martinez FO, Al-Mossawi MH, de Wit J, Vecellio M, et al. CBP30, a selective CBP/p300 bromodomain inhibitor, suppresses human Th17 responses. *Proc Natl Acad Sci U S A.* 2015;112(34):10768–73.
41. Mazur PK, Herner A, Mello SS, Wirth M, Hausmann S, Sanchez-Rivera FJ, Lofgren SM, Kuschma T, Hahn SA, Vangala D, et al. Combined inhibition of BET family proteins and histone deacetylases as a potential epigenetics-based therapy for pancreatic ductal adenocarcinoma. *Nat Med.* 2015;21(10):1163–71.
42. Raraty MG, Murphy JA, McLoughlin E, Smith D, Criddle D, Sutton R. Mechanisms of acinar cell injury in acute pancreatitis. *Scand J Surg.* 2005;94(2):89–96.
43. Ferri-Borgogno S, Barui S, McGee AM, Griffiths T, Singh PK, Pieltz CG, Ghosh B, Bhattacharyya S, Singhi A, Pradhan K, et al: **Paradoxical Role of AT-rich Interactive Domain 1A in Restraining Pancreatic Carcinogenesis.** *Cancers (Basel)* 2020, 12(9).
44. Zhang Y, Yan W, Collins MA, Bednar F, Rakshit S, Zetter BR, Stanger BZ, Chung I, Rhim AD, di Magliano MP. Interleukin-6 is required for pancreatic cancer progression by promoting MAPK signaling activation and oxidative stress resistance. *Cancer Res.* 2013;73(20):6359–74.
45. Ancrile B, Lim KH, Counter CM. Oncogenic Ras-induced secretion of IL6 is required for tumorigenesis. *Genes Dev.* 2007;21(14):1714–9.
46. Chen F, Li X, Aquadro E, Haigh S, Zhou J, Stepp DW, Weintraub NL, Barman SA, Fulton DJR: **Inhibition of histone deacetylase reduces transcription of NADPH oxidases and ROS production and ameliorates pulmonary arterial hypertension.** *Free Radic Biol Med.* 2016 Oct;99:167–178..

Tables

Due to technical limitations, table 1 is only available as a download in the Supplemental Files section.

Figures

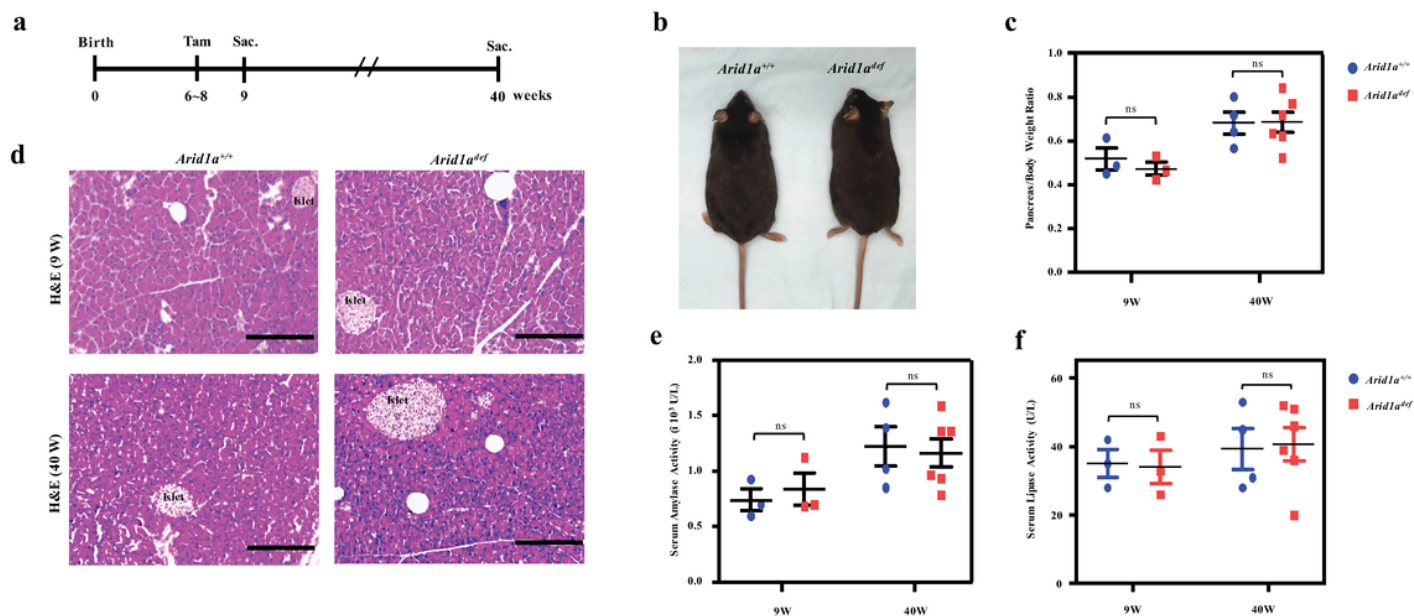


Figure 1

Conditional acinar-specific *Arid1a* knockout mice display the normal pancreas. (a) Scheme for tamoxifen (Tam) administration and then pancreata and blood sampling for mice euthanized at 9-week and 40-week old, respectively. (b) Representative gross photograph of *Arid1a*^{+/+} and *Arid1a*^{Δf} mice of 40-week old. (c) Pancreas/body weight ratio (%) at 9-week (n= 3 *Arid1a*^{+/+} and 3 *Arid1a*^{Δf} mice) and at 40-week old (n= 4 *Arid1a*^{+/+} and 6 *Arid1a*^{Δf} mice). (d) H&E staining of pancreata from *Arid1a*^{+/+} and *Arid1a*^{Δf} mice. Scale bars represents 100 μm. (e-f) the serum amylase and lipase levels of *Arid1a*^{+/+} and *Arid1a*^{Δf} mice. Data are represented as means ± SEM (n = 3 *Arid1a*^{+/+} and 3 *Arid1a*^{Δf} mice at 9-week; n = 4 *Arid1a*^{+/+} and 6 *Arid1a*^{Δf} mice at 40-week). ns, not significant.

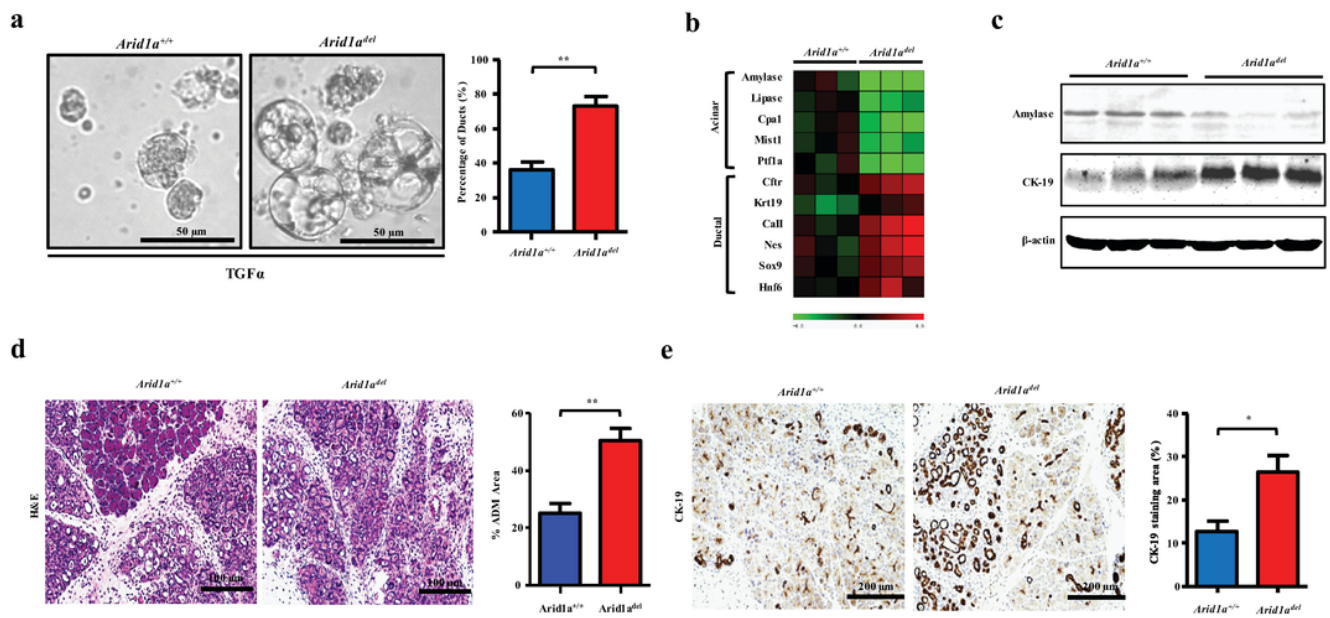


Figure 2

Arid1a deficiency promotes ADM formation ex vivo and in vivo. (a) Primary acinar cells from *Arid1a*^{+/+} and *Arid1a*^{Δ/Δ} mice were seeded into pre-coated 6-well plate. At day 5, ring-like spheres were counted to evaluate percentage of ADM events, and statistical significance of differences between two groups was analyzed (n = 3 per group) as shown in the right panel. Scale bar, 50 μm. (b) Heatmap showing qPCR analysis of acinar/ductal cell markers in primary acinar explants isolated from *Arid1a*^{+/+} and *Arid1a*^{Δ/Δ} mice. (c) Western blot assay of amylase, and CK-19 expression in ex vivo acinar explants. (d) Representative H&E staining on pancreata from (n= 5 *Arid1a*^{+/+} and 7 *Arid1a*^{Δ/Δ} mice) 1 week after cerulein treatment. (e) IHC assay for the duct marker CK-19 in AP model from *Arid1a*^{+/+} and *Arid1a*^{Δ/Δ} mice. Scale bars: 200 μm. Quantification of CK-19 stained area was shown and analyzed statistically. *, p < 0.05; **, p < 0.01;

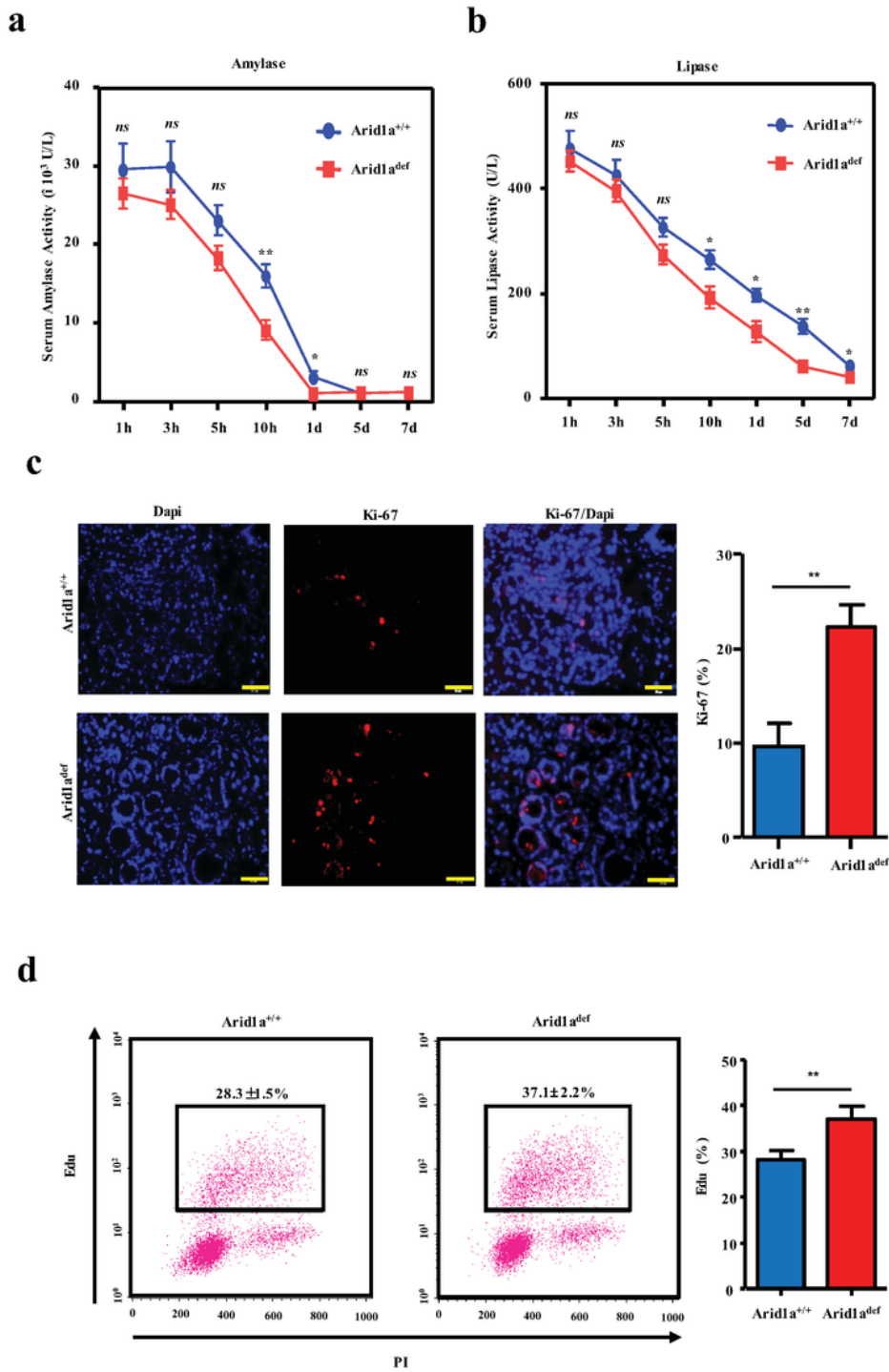


Figure 3

Arid1a deficiency disrupts the normal function and promotes cell proliferation of acinar cells in AP model. (a-b) Serum amylase and lipase activity were measured in Arid1a^{+/+} and Arid1a^{def} mice at indicated time points after the cerulein treatment. (c) Immunofluorescence for Ki-67 (red) expression reflecting proliferative index on pancreata tissue from AP mice 1 week after cerulein injection. Nuclei are labeled with DAPI (blue). Scale bars: 50 μ m. Quantification and statistical analysis of Ki-67 stained nuclei

between two groups were shown in the right histogram (n = 3 Arid1a^{+/+} and 4 Arid1a^{def}). (d) Primary acinar cells were cultured in the collagen/waymouth media mixture for 3 days, followed by 10 μ M EdU treatment for 12h. Single cell suspensions were prepared by collagenase and trypsin digestion from the cultured acinar cells ex vivo. Flow cytometry analysis of Edu-positive cells representing S-phase cells, percentage of Edu-positive cells was shown in the right histogram (mean \pm SEM). *, p < 0.05; **, p < 0.01; ns, not significant.

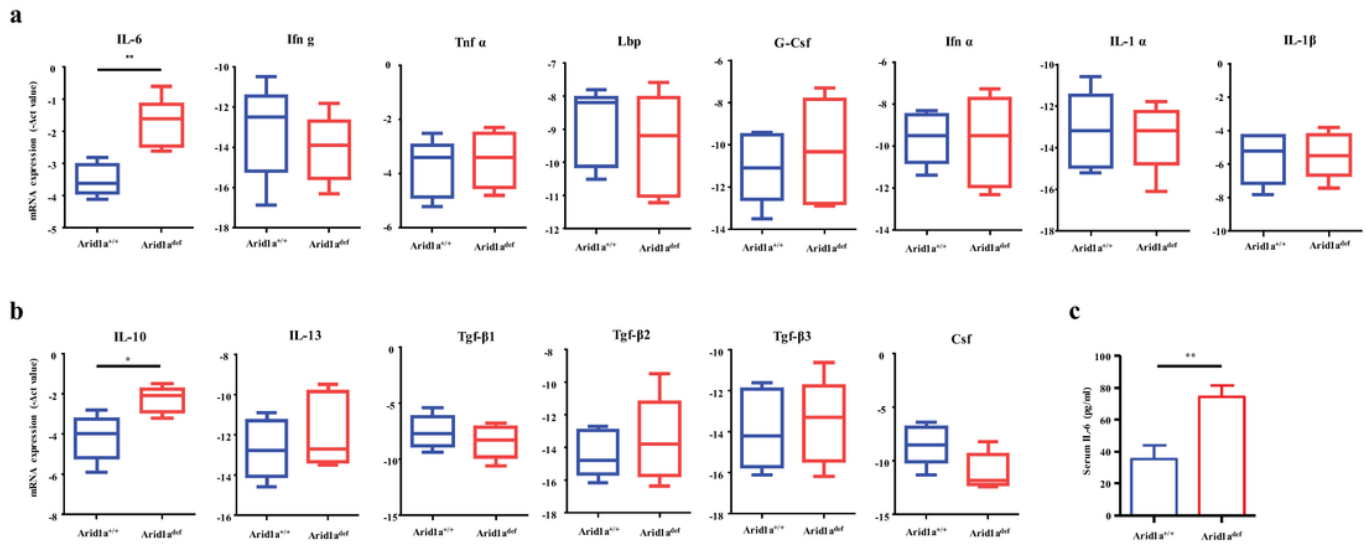


Figure 4

Effects of Arid1a deficiency on proinflammatory and anti-inflammatory cytokine expression in AP tissue from Arid1a^{+/+} and Arid1a^{def} mice. (a-b) qRT-PCR analysis of mRNA levels of the proinflammatory cytokines Ifng, Tnf α , Lbp, G-Csf, Ifn α , IL-1 α , and IL-1 β (a) and the anti-inflammatory cytokines IL-10, IL-13, Tgf β 1-3 and Csf (b) from pancreatic tissue of Arid1a^{+/+} and Arid1a^{def} mice harvested 1 week following caerulein-induced injury. Housekeeping gene Rpl13a was used to normalized gene expression level in AP tissues. Normalized data are displayed in the scatter with mean \pm SEM. (c) Serum levels of IL-6 was measured in Arid1a^{+/+} and Arid1a^{def} mice (n = 5 Arid1a^{+/+} and 5 Arid1a^{def}). *, p < 0.05; **, p < 0.01, unpaired Student's t-test.

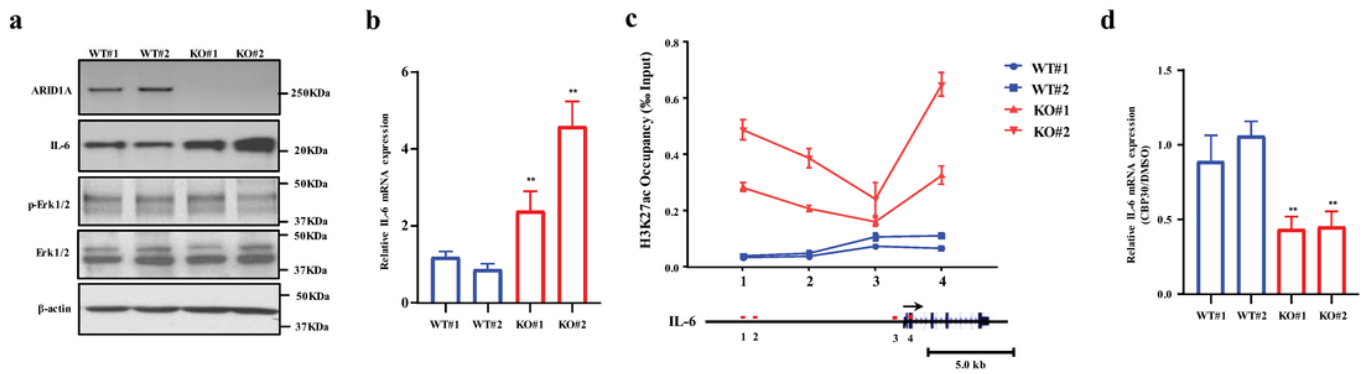


Figure 5

ARID1A deficiency leads to IL-6 upregulation via remodeling H3K27ac modification at its regulatory region. (a) Western blot assay of ARID1A, IL-6, p-Erk1/2, Erk1/2, and loading control β -actin in CRISPR/Cas9-mediated isogenic cell models of human HPNE expressing KRAS mutant (KRASG12D), where 2 WT and 2 KO subclones were used in this assay. (b) IL-6 mRNA levels were validated by qPCR in the same cell lines model. Schematic diagram of IL-6 gene loci for ChIP analysis shown as below, where transcription start site (TSS) was indicated by arrows and amplicons were positioned with red lines. Scale bar, 5.0 kb. (c) ChIP-qPCR analysis showed that ARID1A knockout increased K3K27ac modification at distal and proximal regions of IL-6 gene. (d) These cells were treated with a HAT inhibitor CBP30 (5 μ M), and then qPCR was performed to determine IL-6 expression change relative corresponding DMSO control. Data were shown as means \pm SD, **, $p < 0.01$.

Supplementary Files

This is a list of supplementary files associated with this preprint. Click to download.

- [Version1SupplementaryTable1.xlsx](#)
- [Zhangetal.FigS1.ai](#)
- [Zhangetal.FigS2.ai](#)
- [Zhangetal.FigS3.ai](#)
- [Zhangetal.FigS4.ai](#)